

Research Journal of Pharmaceutical, Biological and Chemical Sciences

Molecular Docking Study on Xanthone Derivatives toward Alpha-Glucosidase.

Saoussen LAKEHAL^a, Fouad FERKOUS^a, Khairedine KRAIM^{a,b}, Ouassila ATTOUI YAHIA^a, and Youcef SAIHI^{a*}.

^aLCOA : Laboratoire de Chimie Organique Appliquée, Département de Chimie, Faculté des Sciences, Université Badji-Mokhtar, BP 12 Annaba, Algérie.

^bENSET : Ecole Normale Supérieure d'Enseignement Technologique, Azzaba, Skikda, Algérie.

ABSTRACT

In this work, a total of 189 xanthone derivatives were selected for molecular screening. These molecules are selected based on a literature research on natural compounds with inhibitory activity against alpha-glucosidase. Molecular docking analysis was carried out, using Molegro Virtual Docker to screen the 189 xanthone derivatives into active site of NtMGAM obtained from X-ray crystal structure 3w4I.PDB. It revealed that a number of sulfonamide xanthone derivatives have presented better energy values than the co-crystallized ligand "Miglitol", and can interact with catalytic residues, thus making them, possible catalytic inhibitors against NtMGAM.

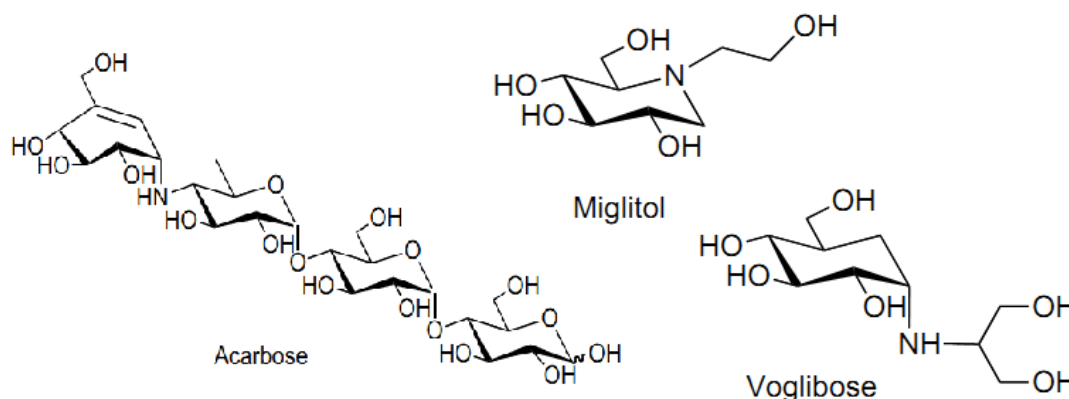
Keywords: Molecular docking, virtual screening, xanthone derivatives, alpha-glucosidase, inhibition, NtMGAM.

**Corresponding author*

INTRODUCTION

Inhibition of alpha glucosidase in the digestive tract constitutes a promising therapeutic class against diabetic disease (Type II), by reducing the rate of glucose absorption, and consequently suppresses the levels of postprandial blood glucose and insulin.[1]

Bioactive components isolated from medicinal plants that are used in traditional medicine often provide the lead structures for modern drug research and development strategies. Therefore, much effort has been expended in the search for effective and safe based on natural materials for use as antidiabetic agents.[2, 3] All α -glucosidase inhibitors marketed as antidiabetic drugs are sugar mimics such as acarbose, miglitol and voglibose .[4] (**Scheme 1**)



Scheme 1. Structures of sugar mimics α -glucosidase inhibitors currently used as anti-hyperglycemic drugs: acarbose; miglitol and voglibose

More attention is devoted to develop new α -glucosidase inhibitors based on non-sugar mimic scaffolds.[5] Recently, xanthone and its derivatives, readily isolated from some medicinal plants, have demonstrated their potential to become a lead drug candidate due to their multiple pharmacological properties including antiinflammatory, antithrombotic, antitumor effects.[6-9]

Due to their unique structural features with a tricyclic scaffold, several computational and experimental studies have been conducted and present xanthone derivatives as promising α -glucosidase inhibitors.[10-16] In the present work, docking-based screening protocol for xanthone-based library toward α -glucosidase is presented. We postulated that ligand docking could be complemented with additional binding site information derived from enzyme-ligand interaction. The screening is followed by ranking of the in-house xanthone library and the analysis of the residues-xanthone derivatives interactions.

MATERIALS AND METHODS

Target Enzyme

Human Maltase Glucoamylase intestinal from Humosepien (MGAM) was selected as α -glucosidase target enzyme. The crystal structure of the target MGAM was retired from the Protein Data Bank (PDB) at the Research Collaborator for Structural Bioinformatics (www.rcsb.org). The selected Pdb (ID:3L4W) represent the crystal structure of MGAM in complex with the potent inhibitor miglitol with a resolution of 1.90Å, while the miglitol ,which was identified as one of the potent inhibitors of α -glucosidase [17].

Preparing the library of xanthone derivatives

As mentioned above, we have selected the natural product xanthone as scaffold, thus a library in size of 189 xanthone derivatives was collected from the literature. In order to ensure the presence of the different interactions (hydrophobicity, nucleophilicity, Van Der Waals, steric interactions) in the complex xanthone derivative – α -glucosidase enzyme (binding site), the in-house library is rich in terms of function diversity on

the structure of the xanthone scaffold. The molecular structures in the set were crocked and optimized using hyperchem 8.0. The whole 3D structures of dataset are presented in the "supplementary data materials".

Molecular docking simulation

We have adopted the molecular docking approach to exploit the effect of structure – relationship of xanthone derivatives on the inhibition of α -glucosidase enzyme and consequently to interpret the different interactions types resulted from the process of inhibition. Therefore, this approach allows us ranking the whole xanthone derivatives according to their energies of interactions with the target binding site.

This study was performed using Molegro Virtual Docker (MVD 2012.5.5.0, Molegro ApS), which is based on heuristic search algorithm that combines differential evolution with the cavity prediction algorithm which has been successfully applied to molecular docking simulation [18, 19]. MVD program exhibits superior overall performance in comparison with other popular programs like Autodock, Superflex, Flex and Gold.[20-23] After molecular docking simulation process, results are stored and visualized with PyMol molecular visualization tool. [24]

Molecular docking work-space preparation

For our target complex (PDB ID:3L4W), water molecules were excluded; the rotatable bonds of the ligands were set to be free; the enzyme was considered as a rigid body; hydrogen atoms were added and MDV default charges were assigned; molecular cavities were detected using the grid-based prediction algorithm and all atoms types and bond orders were corrected to both ligand and enzyme using MVD automatic preparation functions [20].

Protocol validation test

This procedure called "re-docking" is a validation method in order to determines the ability of docking algorithm to recover the crystallographic position using docking simulation, the best binary complex is the one which has a geometric conformation closer to the crystallographic structure. For that reason, we have used the root-mean-square deviation (RMSD) calculation, which is calculated between two sets of atomic coordinates ($x_{crystal}$, $y_{crystal}$, $z_{crystal}$: crystallographic structure atomic coordinates; x_{poses} , y_{poses} , z_{poses} : predicted model atomic coordinates; N: atoms being compared) in order to determine the distance from the docking-generated solution (pose) to the original crystallographic structure (**equation 1**). It is expected that the best docking results generate RMSD values less than 2.0 Å compared with original crystallographic structures.[25]

$$RMSD = \sqrt{\frac{1}{N} \left((x_{crystal} - x_{poses})^2 + (y_{crystal} - y_{poses})^2 + (z_{crystal} - z_{poses})^2 \right)} \quad (1)$$

To validate our protocol, we used the MGAM crystallographic structure with a PDB ID: 3L4W, we performed a docking protocol into the active site of MGAM and compared the docked pose with the original structure.

During the research process, the docking applied protocol was carried out in a search space at coordinates: x=45.21, y=92.20, z=34.87 and a docking sphere radius of 15Å (**Figure 1**). All water molecules were deleted from original PDB file. There for, the search space covered all the amino acid residues in considered active site.

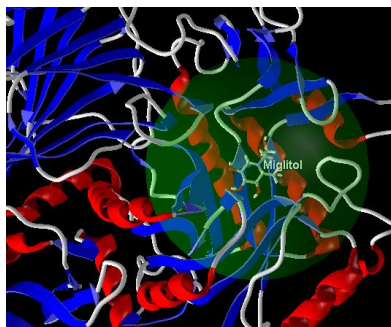


Figure 1. Search space sphere (green) used for molecular docking simulation

MDV presents biological inspired algorithm to perform positional searches in docking procedure. For our protocol we used the MolDock Optimizer as search algorithm which is based on a GDEA (Guided differential evaluation algorithm) and MolDock Score [Grid] as scoring function in order to cluster best binding energy solutions.

Docking-based virtual screening protocol

Once the docking protocol is chosen and validate (RMSD < 2Å obtained from re-docking step), a typical docking simulation was performed for each ligand present in our xanthone derivatives in-house library using MolDock Optimizer as search algorithm and MolDock Score as scoring function.

The MolDock Optimizer search algorithm used in MVD is inspired by Darwinian evolution theory. Compared to more widely known EA-based techniques (e.g. genetic algorithms, evolutionary programming, and evolution strategies), MolDock Optimizer search algorithm is a guided differential evolution algorithm (DE) which uses a different approach to select and modify candidate solutions (individuals). The main innovative idea in DE is to create offspring from a weighted difference of parent solutions.[20]

During docking simulation several poses (binding orientations and conformations) can be obtained for each ligand, here we select the best poses from the lowest binding energy solutions clustered by MolDock Score [Grid] as a grid-based score function precalculates potential-energy values on an evenly spaced cubic grid in order to speed up calculations. This scoring function which is derived from PLP scoring functions originally proposed by Gehlhaar et al [26, 27]. and later extended by Yang et al[28, 29].

The MolDock Score docking scoring function, $E_{MolDock\ Score}$, is defined by the following energy terms:

$$E_{MolDock\ Score} = E_{inter} + E_{intra} . \quad (2)$$

Where the E_{inter} is the enzyme–ligand interaction energy:

$$E_{inter} = \sum_{i \in ligand} \sum_{j \in protein} \left[E_{PLP} (r_{ij}) + 332.0 \frac{q_i q_j}{4r_{ij}^2} \right] \quad (3)$$

Where:

- E_{PLP} : Piecewise linear potential.
- The electrostatic interactions between charged atoms are described by the second term.
- The numerical value of 332.0 fixes the units of the electrostatic energy in kcal/mol.

The E_{intra} is the internal energy of the ligand:

$$E_{intra} = \sum_{i \in ligand} \sum_{j \in ligand} E_{PLP}(r_{ij}) + \sum_{flexible\ bonds} A[1 - \cos(m.\theta - \theta)] + E_{clash} \quad (4)$$

Where:

- The first term calculates all the energies involving pairs of atoms of the ligand, except those connected by two bonds.
- The second term refers to the torsional energy with θ is the torsional angle of the bond
- E_{clash} : assigns a penalty of 1000 if the distance between two heavy atoms is smaller than 2.0 Å.

The optimized parameters for our docking simulation are the following:

- search space coordinates : x=45.21, y=92.20, z=34.87 , docking sphere radius of 15Å
- Search algorithm: MolDock Optimizer
- Scoring function :MolDock Score [Grid]
- Number of runs: 100
- Max population size : 150
- Max iterations : 2000
- Scaling Factor : 0.5
- Crossover rate : 0.9

RESULTS AND DISCUSSION

Our virtual screening is based on the crystallographic structure information of the target α -glucosidase (MGAM: EC 3.2.1.20) which make part of the glycosyl hydrolase family 31 (GH31) and operate through a configuration-retention catalytic mechanism via the classical Kosland hydrolyse mechanism involving a nucleophilic attack and a base-catalyzed hydrolysis by a catalytic nucleophil residue and an acid/base catalyst residue respectively, resulting in the release and net retention of the anomeric configuration of the product.[30]

Mutagenesis studies on NtMGAM along with substrate trapping studies and sequence alignments on GH31 members have identified Asp443 as the catalytic nucleophile and the Asp542 as the acid/base catalytic residues.[31, 32] according to those studies, crystallographic studies of MGAM in complex with potent inhibitors like acarbose and miglitol have been reported in order to take a closer look into the inhibition mechanism.[33, 34] It is reported that these selective inhibitor of ntMGAM interacts through hydrogen bonding interactions with Asp327, His600, Asp542 and the catalytic nucleophile Asp443. In this work, we selected the MGAM as a target enzyme in complex with miglitol (PDB Id: 3L4W)

Re-docking validation step

The re-docking step which represents the first step in the virtual screening protocol, is realized using the structure of NtMGAM in complex with Miglitol (3L4W). The re-docking simulation generated an RMSD of 0.3 Å, this result indicated that the present docking protocol was successful and can be applied for next steps.

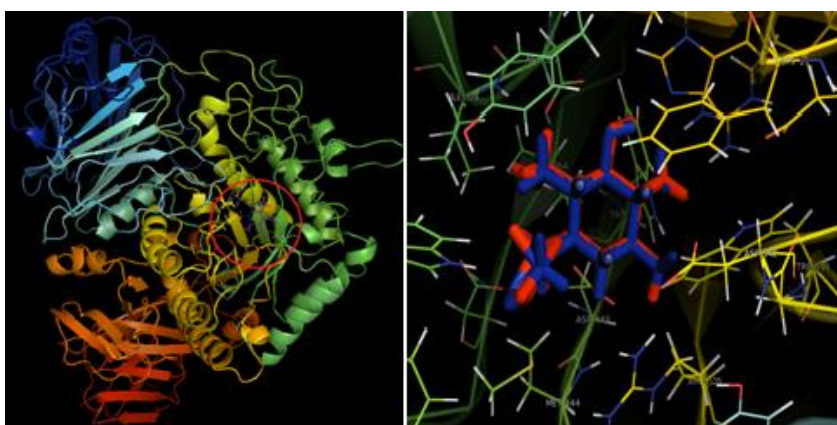


Figure 2. The superposition of the best docked pose of Miglitol (colored by red) with the corresponding to the X-ray original conformation (colored by blue), RMSD =0.3Å

Taking a closer look into the residues in interaction with the docked pose (**Figure 3**), we could note that this pose interacts likely with the same manner as the original crystallographic ligand, through hydrogen bonds with the residues: Asp 327, His 600, Arg526, the catalytic nucleophile Asp 443 and the acid/base catalyst Asp542.

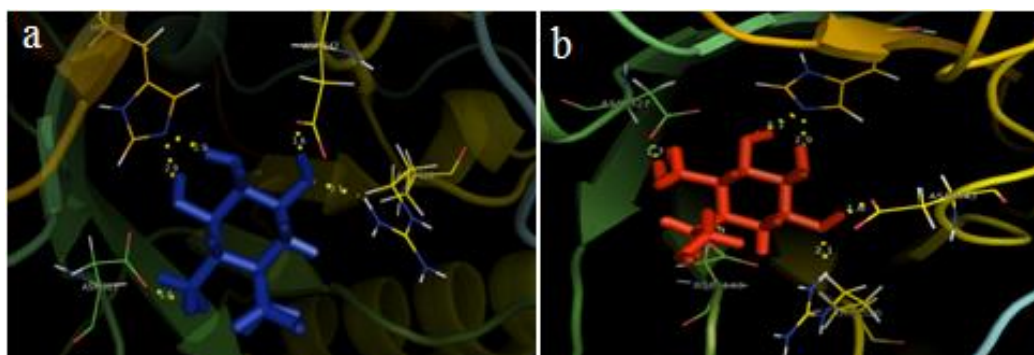


Figure 3. Miglitol original x-ray binding mode with neighboring residues (a). Miglitol best docking-generated solution (pose) binding mode with neighboring residues (b).

Molecular-based Virtual screening

Application of the previously described docking protocol to our in-house database with 189 xanthone derivatives returns a set of 20 top-scoring compounds (**Scheme 2**) starting from their most promising docking poses obtained from 100 independent docking runs within the defined binding site. Therefore, ligand–protein interaction energies were calculated in order to get a better understanding about the binding mode for each selected compound with binding site neighboring residues.

Table 1. MolDock Score, Hbond Score and VDW contacts binding energies estimate of miglitol and the twenty top-scoring xanthone derivatives obtained from molecular docking simulaton.

| Ligand | Moldock Score (Kcal/mol) | Hbond Score (Kcal/mol) | VDW (Kcal/mol) |
|----------|--------------------------|------------------------|----------------|
| Miglitol | -81.747 | -17.684 | -24.123 |
| X170 | -151.543 | -21.8045 | -39.408 |
| X117 | -149.164 | -6.3648 | -53.0356 |
| X103 | -143.448 | -7.63514 | -48.5584 |
| X138 | -140.546 | -6.87024 | -54.0503 |
| X120 | -138.459 | -3.51585 | -17.657 |
| X156 | -136.894 | -17.0098 | -15.9694 |
| X47 | -136.033 | -8.82717 | -45.187 |
| X111 | -135.549 | -5.95684 | -17.7255 |
| X113 | -135.197 | -8.62535 | -51.6191 |
| X161 | -134.515 | -19.0537 | -34.748 |
| X108 | -133.964 | -6.80362 | -49.0377 |
| X112 | -133.583 | -11.0071 | -53.647 |
| X110 | -133.411 | -5.08771 | -50.5477 |
| X105 | -132.543 | -6.15226 | -47.8284 |
| X107 | -128.99 | -7.89712 | -44.7367 |
| X102 | -128.323 | -4.98946 | -47.9053 |
| X109 | -127.288 | -7.77745 | -42.9553 |
| X114 | -126.51 | -5.28926 | -44.4706 |
| X168 | -124.736 | -19.1923 | -12.2206 |
| X155 | -124.574 | -19.9812 | -31.3819 |

According to Moldock Score values (**Table1**), we can observe clearly that all 20 top-scoring xanthone derivatives show a good ligand-enzyme affinity with binding energy values ranging from -151.543 kcal/mol to -124.574 kcal/mol, while the miglitol moldock score is equal to -81.747, which can enable these molecules to be energetically competitive to miglitol. Another interesting finding that out the twenty top-scoring ligands, eighteen compounds are xanthone sulfonamides derivatives which may represent a new class of α -glucosidase inhibitors. For our best knowledge, no studies have been reported previously their inhibitory activity toward the target enzyme NtMGAM.

Docking simulation results exhibit that the two top scored poses x170 and x117 are xanthone sulfonamide derivatives, showed good binding energy (Moldock score) of -151.543 and -149.164 Kcal mol⁻¹ respectively.

Interestingly, significant H-bonding interactions were detected in X170- NtMGAM complex (H-bond score of -21.80 Kcal mol⁻¹), where X170 hydroxyl groups have been obviously involved (**Figure 4**): X170-O4 with Gln603-carbonyl backbone and Gln603-NH (O-O: $d= 2.3 \text{ \AA}$ and O-N: $d= 2.8 \text{ \AA}$ respectively); X170-O3 and Gln603-carbonyl backbone (O-O: $d= 2.6 \text{ \AA}$); X170-O5 and Thr205-OH (O-O: $d= 2.7 \text{ \AA}$); X170-O6 and Asp203-CO₂H (O-O: $d= 2.0 \text{ \AA}$); X170-O7 (sulfonamide group) and Arg526-NH₂ (O-N: $d= 2.1 \text{ \AA}$) . Van der Waals contacts were also present between the X170 and Trp406, Tyr605, Ala576 residues.

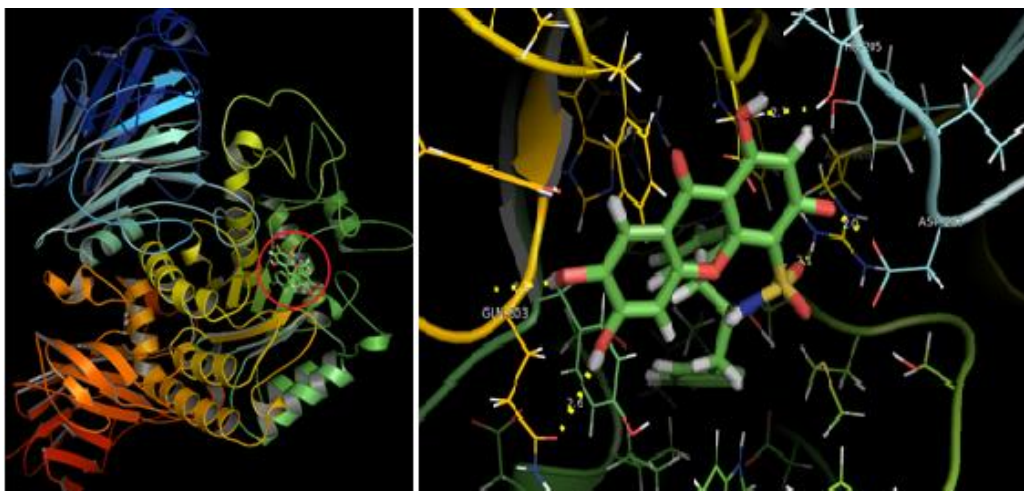


Figure 4. X170 H-bonding interactions with neighboring binding site residues Arg526, Asp203, Thr205 and Gln603.

In X117-MGAM complex, three putative H-bonding interactions were detected (**Figure5**): X117-O4 and Trp406-NH (O-N: $d= 2.5 \text{ \AA}$); X117-O7 (sulfonamide group) and Thr205-OH (O-O: $d= 2.3 \text{ \AA}$); X117-N1 (sulfonamide group) and catalytic Asp542-CO₂H (N-O: $d= 1.8 \text{ \AA}$). Van der Waals contacts were less present in X117- NtMGAM complex: Phe450 and Phe575.

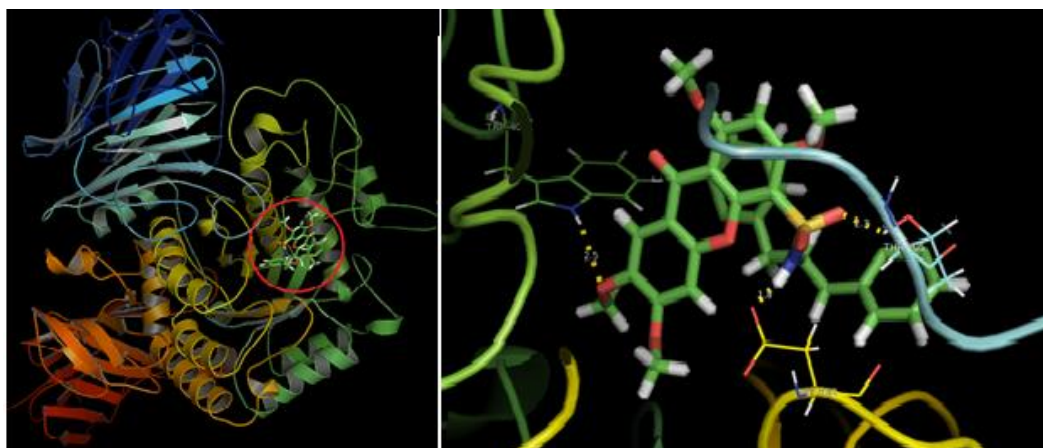


Figure 5. X117 H-bonding interactions with neighboring binding site residues Arg526, Asp203, Thr205 and Gln603.

Table 2. Intermolecular interactions for the 20 top-scoring ligands selected from the molecular docking simulation. H_{Bond} and VDW mean hydrogen bonds and means Van der Waals contacts respectively.

| Residues | Top-scoring Ligands | | | | | | | | | | | | | | | | | | | |
|-------------------|---------------------|------|------|------|------|------|-----|------|------|------|------|------|------|------|------|------|------|------|------|------|
| H _{Bond} | X170 | X117 | X103 | X138 | X120 | X156 | X47 | X111 | X113 | X161 | X108 | X112 | X110 | X105 | X107 | X102 | X109 | X114 | X168 | X155 |
| Asp327 | | | | XX | | | XX | | | | | | | | | | | | | |
| His600 | | | | | | | X | | | | | | | | | | | | | |
| Asp542 | | X | | X | X | XX | | X | | X | X | | | | X | | X | X | XX | |
| Asp443 | | | | | | | | | | | | | | X | | | | | | |
| Arg526 | X | | | X | | | X | | | | | X | | | | | | | | |
| Trp406 | | X | | X | | | X | | | | | | | | X | | X | X | | |
| Thr205 | X | X | X | | X | X | | X | X | X | X | X | X | XX | X | X | X | X | XX | XX |
| Gln603 | XX | | X | | X | XX | | X | | XX | | | | | | | | | X | XX |
| Asp203 | X | | | | | | | | | | | | | | | | | | | |
| Tyr605 | | | X | | | X | | | XX | XX | | X | X | | | | | | XX | XX |
| Tyr299 | | | X | | | X | X | X | X | XX | | X | | | | | | | XX | XX |
| Tyr214 | | | | | | | | | | | X | | | | X | X | X | | | |
| Arg202 | | | | | | | | | | | | | | X | | | | | | |
| VDW | | | | | | | | | | | | | | | | | | | | |
| Trp406 | X | | X | X | X | | X | X | X | X | X | X | | | | | | X | | X |
| Met444 | | | X | X | | X | | X | | | | | | | | | | | | |
| Phe450 | | X | | | | | X | | | | X | | | | X | | X | X | | |
| Phe575 | | X | X | | X | X | | X | | X | | | | | | | | | X | X |
| Thr205 | | | X | | | X | | | | | | X | X | X | | X | | | | |
| Tyr605 | X | | X | X | X | X | | | | X | | | | | | | | | X | X |
| Ala576 | X | | | | | X | | | | X | | | X | | | | | | X | |
| Tyr299 | | | | | | X | | X | | | | | | | | | | | | |
| Ser448 | | | | | | | X | | | | | | | | | | | | | |
| Trp441 | | | | | | | X | X | X | | | | | | | | | | X | |
| Tyr214 | | | | | | | | | | | X | | X | | | | | | | |

Note. The presence of an X indicates that the interaction occurs, while an XX indicates that the ligand have more than one Hydrogen bond with the same residue

It is noteworthy that compounds X170 and X117 have different binding modes although their structure similarity. On the contrary, the absence of hydroxyl groups in X117 did not prevent H-bonding interactions to occur, due to the presence of sulfonamide group which perform two interesting intermolecular hydrogen bonds with Thr205 and catalytic residue Asp542, indicating that sulfonamide group have obviously attributed to establish good binding affinity in the complex.

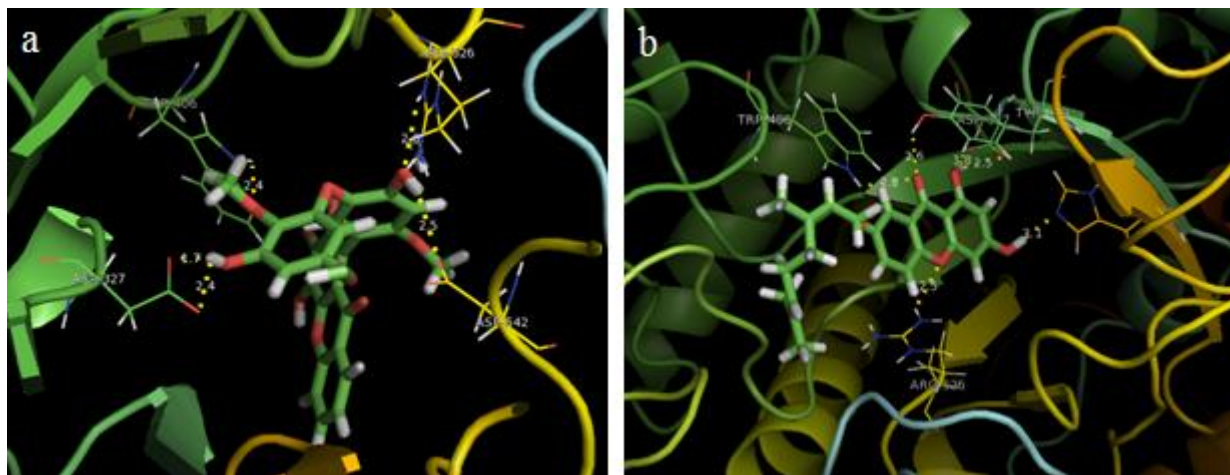


Figure 6. Detected X138 H-Bonds with neighboring residues (a). Detected X47 H-Bonds with neighboring residues (b).

As mentioned previously, out the twenty top-scoring ligands, only two compounds are non xanthone sulfonamides derivatives X138 and X47. Comparing H-bonding interactions in X138-NtMGAM and X47-NtMGAM complexes (Figure 6), binding site residues Asp327, Trp406 and Arg526 were found in interaction with both ligands X138 and X47. It is noticeable that X138 and X47 form H-bonds with catalytic key residues Asp542 and His600 respectively. Van der Waals contacts have also been detected in both complexes (Table 2). Intermolecular interactions for all twenty top-scoring xanthone derivatives all are clustered in Table 2.

Concerning the other top-scoring xanthone sulfonamide derivatives in complex with NtMGAM, similar behaviors were observed due to the occurrences of some interactions in common (Table 2). Analyzing H-bonding interactions, ten ligands perform interesting intermolecular H-bond with catalytic residue Asp542, while H-bond interaction with Thr205 occurs in all the complexes. In addition, H-bond interactions with Tyr299, Tyr605 and Gln603 residues take place in the majority of complexes. Furthermore, interesting VDW contacts with catalytic site residues were found which contributed to establish good binding affinity in all complexes. Therefore, the binding of top-scoring xanthone derivatives with binding site residues would further the blockage of the binding site (Figure 7).

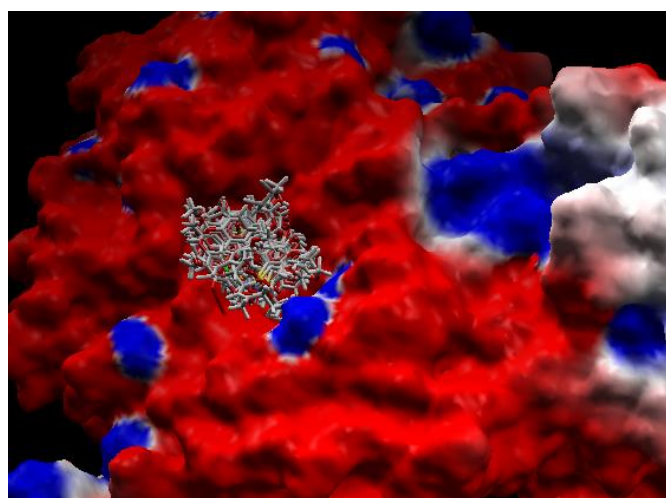
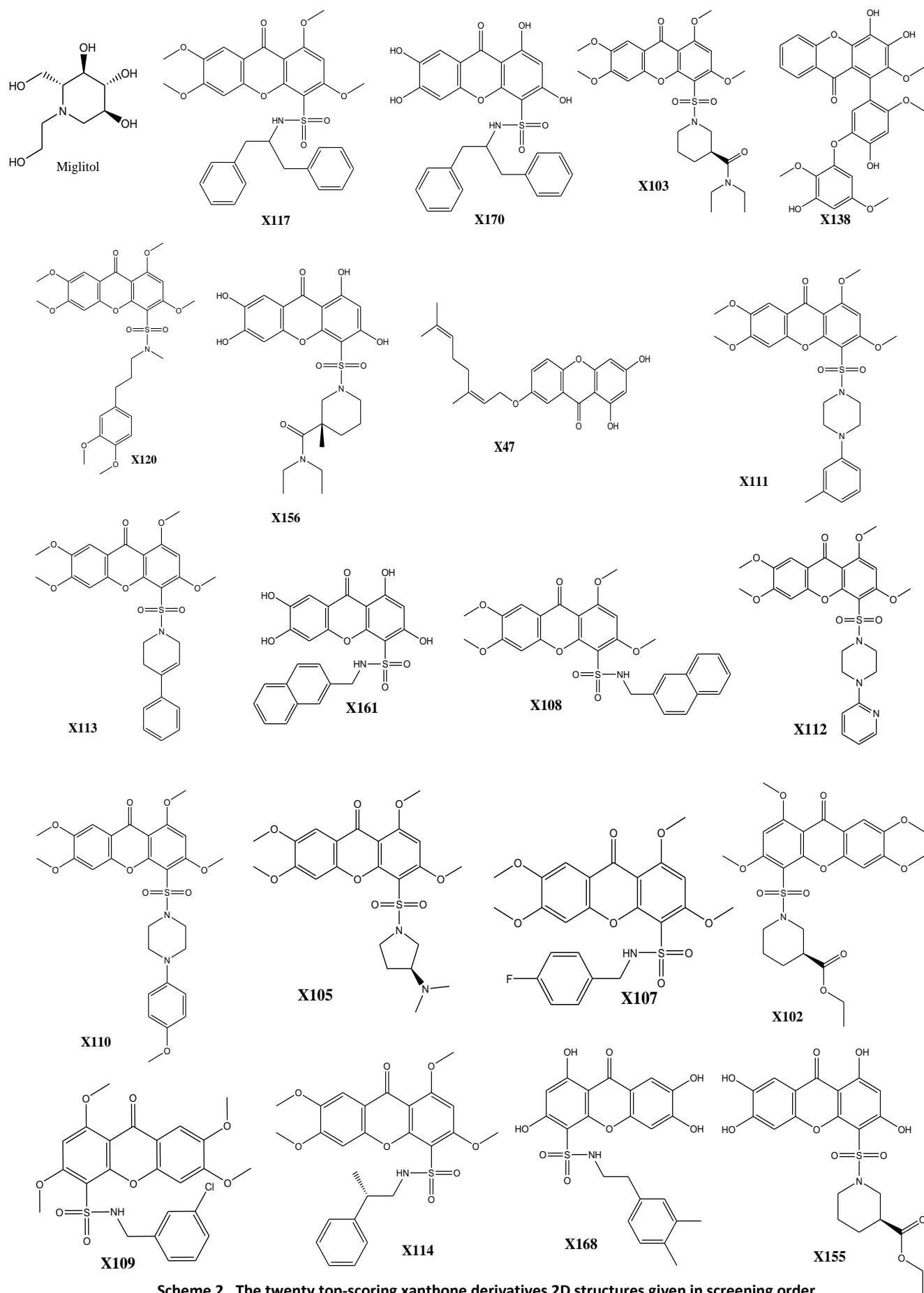


Figure 7. 20-top scoring docking poses relative to NtMGAM binding site surface



Scheme 2. The twenty top-scoring xanthone derivatives 2D structures given in screening order

CONCLUSION

Molecular docking simulation approaches are commonly used in modern drug design process to take a closer look into ligand-receptor binding mode and provide guidance for future studies. In this aim, we have carried out a docking-based virtual screening on an in-house database of 189 xanthone derivatives to provide insights into the binding mechanism at molecular level toward NtMGAM based on crystallographic structure information. This study was performed using Molegro Virtual Docker (MDV) with a combination of MolDock Optimizer as a differential evolution algorithm and MolDock Score scoring function, this combination was validated with Re-docking simulation (RMSD of 0.3 Å).

Binding mode Analysis of each selected 20 top-scoring xanthone derivative against NtMGAM defined binding site revealed that: xanthone derivatives showed favorable binding affinity in comparison with miglitol; key catalytic residues occur significant H-bonding interactions with xanthone derivatives and interesting VDW contacts with catalytic site residues contributed to establish good binding affinity. Thus, similar binding behaviors were observed due to the occurrence of some important H-bonding interactions and VDW contacts in common with NtMGAM binding site residues.

Furthermore, the present work revealed xanthone sulfonamides derivatives as a promising class of α -glucosidase inhibitors, for our best knowledge, no studies have been reported previously their inhibitory activity toward NtMGAM, which is currently under investigation in our laboratory.

ACKNOWLEDGMENTS

This work was generously supported by the General Directorate for Scientific Research and Technological Development (DG-RSDT), Algerian Ministry of Scientific Research. The authors would like to dedicate this work to the memory of their colleague AZZOUZI Abdelkader.

REFERENCES

- [1] Gallienne E, Gefflaut T, Lemaire M. *J Org Chem* **2006**; 71: 894-902.
- [2] Harvey AL, *Drug Discovery Today* **2008**; 13: 894.
- [3] Butler MS. *Nat Prod Rep* **2008**; 25: 475.
- [4] Asano N. *Cell Mol Life Sci* **2009**; 66: 1479 - 1492.
- [5] Eduardo B M, Adriane SG, Ivone C. *Tetrahedron* **2006**; 62: 10277-10302.
- [6] Lin CN, Chung M I, Liou S J, Lee TH, Wang JP. *J Pharm Pharmacol* **1996**; 48: 532-538.
- [7] Lin CN, Hsieh HK, Liou SJ, Ko HH, Lin HC. *J J Pharm Pharmacol* **1996**; 48: 887-890.
- [8] Saraiva L, Fresco P, Pinto E, Sousa E, Pinto M, *Bioorg MedChem* **2002**; 10: 3219-3227.
- [9] Na Y, *J Pharm pharmacol* **2009**; 61: 707-712.
- [10] Kraim K, Khatmi D, Saihi Y, Ferkous F, Brahimi M, *Chemo & Intel Labor Syst* **2009**; 97: 118-126.
- [11] Liu Y, Zou L, Ma L, Chen WH, Wang B, Xu ZL. *Bioorg Med Chem* **2007**; 15: 2810-2814.
- [12] Liu Y, Zou L, Ma L, Chen WH, Wang B, Xu ZL. *Bioorg Med Chem* **2006**; 14: 5683-5690.
- [13] Liu Y, Ke ZF, Cui JF, Chen WH, Wang B. *Bioorg Med Chem* **2008**; 16: 7185-7192.
- [14] Li GL, He JY, Zhang AQ, Wan YQ, Wang B, Chen WH. *Eur J Med Chem* **2011**; 46: 4050- 4055.
- [15] Gao L, Zhou Y, Yan H, Huang F, Wen R, Li G. *Heterocycles* **2011**; 83: 1897-1902.
- [16] Srivastava AK, Pandey A, Nath A, Jaiswal M, Pathak VK. *Oxid Commun* **2010**; 33: 195-204.
- [17] Sim L, Jayakanthan K, Mohan S, Nasi R, Johnston BD, Rose DR. *Biochem* **2010**; 49: 443-451.
- [18] Storn R, Price K. *Global Optim* **1997**; 11: 341-359.
- [19] Thomsen R. *Cogr on evolutionary computation* **2003**, Camberra Australia; 2354-2361
- [20] Thomsen R, Christensen MH, *J Med Chem* **2006**; 11: 3315-3321.
- [21] Heberlé G, De Azevedo WF. *Curr Med Chem* **2011**; 18: 1339 -1352.
- [22] De Azevedo WF. *Curr Drug Targets* **2010**; 11: 327 - 334.
- [23] Araújo JQ, Lima JA, Pinto C, De Alencastro RB, Albuquerque MG. *J Mol Model* **2011**; 17: 1401-1412.
- [24] The PyMol Molecular Graphics system. 1.8 Schrodinger, LLC.
- [25] Friesner RA, Banks JL, Murphy RB, Halgren TA, Klicic JJ. *J Med Chem* **2004**; 47: 1739-1749.
- [26] Gehlhaar DK, Verkhivker G, Rejto PA, Fogel DB, Fogel LJ, ST Freer. *Proceedings of the Fourth International Conference on Evolutionary Programming* **1995**; 615-627.



- [27] Gehlhaar DK, Bouzida D, Rejto PA. Proceedings of the Seventh International Conference on Evolutionary Programming **1998**; 449-461.
- [28] Yang JM. J Med Chem **2004**; 25: 843-857.
- [29] Yang JM, Chen CC. Proteins **2004**; 55: 288-304.
- [30] Koshland DE. Biological Reviews **1953**; 28: 416-436.
- [31] Nichols BL, Avery S, Sen P, Swallow DM, Hahn D. Proc Natl Acad Sci USA **2003**; 3: 1432-1437.
- [32] Lovering AL, Lee SS, Kim YW, Withers SG, Strynadka NC. J BioChem **2005**;3: 2105-2115.
- [33] Ren LM, Qin XH, Cao XF, Wang LL, Bai F. Protein Cell **2011**; 2: 827-836.
- [34] Sim L, Jayakanthan K, Mohan S, Nasi R, Johnston BD, Pinto BM, Rose DR. Biochemistry **2010**;49: 443-451.